EXPERIMENTELLE TECHNIK DER PHYSIK
EXPERIMENTAL TECHNIQUE OF PHYSICS

HERAUSGEGEBEN VON A. LÖSCHE UND E. SCHMUTZER

36. JAHRGANG 1988 HEFT 4/5

Recent Methodical Developments of ENDOR and ODMR in Solids*)

Neuere methodische Entwicklungen bei ENDOR und ODMR in Festkörpern

Новые методические развития двойного электронно-ядерного резонанса (ДЭЯР) и оптического детектирования ЭПР и ДЭЯР в твердых телах

By J.-M. SPAETH, Paderborn

(Received Dec. 3, 1987)

Abstract

Recent developments of ENDOR spectroscopy which are based on computer-aided experiments and analysis of spectra, are reviewed especially in view of their use in materials science. With these techniques and advanced methods like ENDOR-induced EPR and DOUBLE ENDOR, complex defect problems can be solved. Correlation with energy levels is possible by performing photo-ENDOR experiments. The optical detection of EPR and ENDOR (ODEPR and ODENDOR) via the magnetic circular dichroism (MCD) of the optical absorption of defects (intracenter transitions) was recently successfully applied to semiconductors. With an excitation spectroscopy of ODEPR and ODENDOR lines a direct correlation between the optical bands of a defect and its EPR/ENDOR lines becomes possible. ODEPR was also observed in ionizing defect transitions in semiconductors. Correlation to energy levels is possible by photo-ODEPR/ODENDOR experiments. A novel method is described for the determination of defect spin states using their MCD of the absorption.

Zusammenfassung

Es wird ein Überblick über neuere Entwicklungen in der ENDOR-Spektroskopie, die auf rechnergestützten Experimenten und Spektrenanalyse beruhen, besonders im Hinblick auf ihre Verwendung in der Materialwissenschaft, gegeben. Mit diesen Techniken sowie fortgeschrittenen Methoden, wie ENDOR-induzierte EPR und DOPPEL-ENDOR, können komplexe Defektprobleme gelöst werden. Eine Korrelation mit Energie-Niveaulagen ist möglich über Photo-ENDOR-Experimente. Der optische Nachweis von EPR und ENDOR (ODEPR und ODENDOR) über den magnetischen Zirkulardichroismus (MCD) der optischen Absorption (Intrazentren-Übergänge) wurde neuerlich erfolgreich auf Halbleiter angewandt. Mit einer Anregungsspektroskopie von ODEPR- und ODENDOR-Linien wird eine direkte Korrelation zwischen den optischen Banden eines Defektes und seinen EPR/ENDOR-Linien möglich. ODEPR wurde ebenfalls in Ionisationsübergängen von Defekten in Halbleitern beobachtet. Eine Korrelation zu Energie-Niveaulagen ist möglich durch Photo-ODEPR/ODENDOR-Experimente. Eine neuartige Methode wird beschrieben, den Spinzustand von Defekten zu bestimmen über den magnetischen Zirkulardichroismus der Absorption.

*) Lecture at the Magnetic Resonance Conference, held in Reinhardsbrunn, Nov. 9—13, 1987.

1. Introduction

Recent developments in electron nuclear double resonance (ENDOR) and optically detected magnetic resonance (ODMR) spectroscopy, which have been particularly useful for materials science, will be briefly reviewed. Since already small concentrations of defects can decisively influence the bulk properties of materials such as semiconductors or insulating crystals, the microscopic identification of point defects and small clusters of point defects is a very important problem in this field. The determination of the defect structure is based on the measurement of hyperfine (hf) and superhyperfine (shf) interactions. Although ENDOR [1] is known to be the almost only suitable method for defect structure determination by being able to resolve the shf interactions (apart from a few favourable cases, where EPR is sufficient), it has not become a standard and wide spread technique for materials characterization as e.g. photo-luminescence and DLTS (deep level transient spectroscopy) have become in semiconductor physics. The reason may be that there are a number of difficulties associated with its application in materials science. ENDOR spectra easily get very complicated and sensitivity compared to EPR is a problem, since in conventional solid state ENDOR the ENDOR effect is at most of the order of a few percent of the EPR effect. It is usually much less. Recently, considerable progress has been made by introducing computer-aided methods both in the experiment and analysis of spectra, by introducing advanced ENDOR techniques and by optical detection of ENDOR. Furthermore, the correlation of the defect structure as revealed by the EPR/ENDOR spectra with other properties like optical absorption or emission bands or the energy level positions in the gap of the defects investigated provided the necessary link between defect structure and bulk properties of the crystal. In this way ENDOR spectroscopy is a particularly powerful tool for materials science, which is not paralleled by any other method.

The methods described below will be illustrated by examples, which were chosen such as to best illustrate the method and not necessarily to be the most recent ones.

2. Computer-Aided Electron Nuclear Double Resonance

In the stationary ENDOR method [2] the nuclear magnetic resonance (NMR) transitions of nuclei coupled to the unpaired electron of the defect are observed by monitoring the increase of the partially saturated EPR signal upon fulfilling the double resonance condition. This is schematically indicated in Fig. 1 for $S = {}^1/_2$ and one nucleus with $I = {}^3/_2$. In most solids the cross relaxation (T_X in Fig. 1) is operating well enough to allow ENDOR to be observed as a stationary effect [2]. Since ENDOR is at most a small effect of 1···2 % of the EPR signal, mostly much smaller, high sensitivity of the spectrometer is essential as well as the help of any method to improve the signal-to-noise ratio (see below). The use of low noise microwave amplifiers in homodyne spectrometers has made the construction of the complicated superheterodyne spectrometers unnecessary [3].

Each nucleus gives rise to 2 ENDOR lines (for $S = {}^1/_2$), if there is quadrupole interaction this number is multiplied by $2I$. In order to determine the orientation and principal values of the shf and quadrupole interaction tensors and infer from them the defect structure, a complete angular dependence of the spectra has to be measured. As Fig. 2 shows for the comparetively 'simple' defect Ni^{3+} on Ga-site in GaP, many ENDOR lines can occur for each crystal orientation in a narrow frequency range [4]. Very often it is very hard to follow a particular angular dependence for a particular ligand nucleus. Here computer-aided methods have made possible both experiment and the analysis of the spectra. In the computer controlled experiment the ENDOR angular dependence can be measured automatically in small

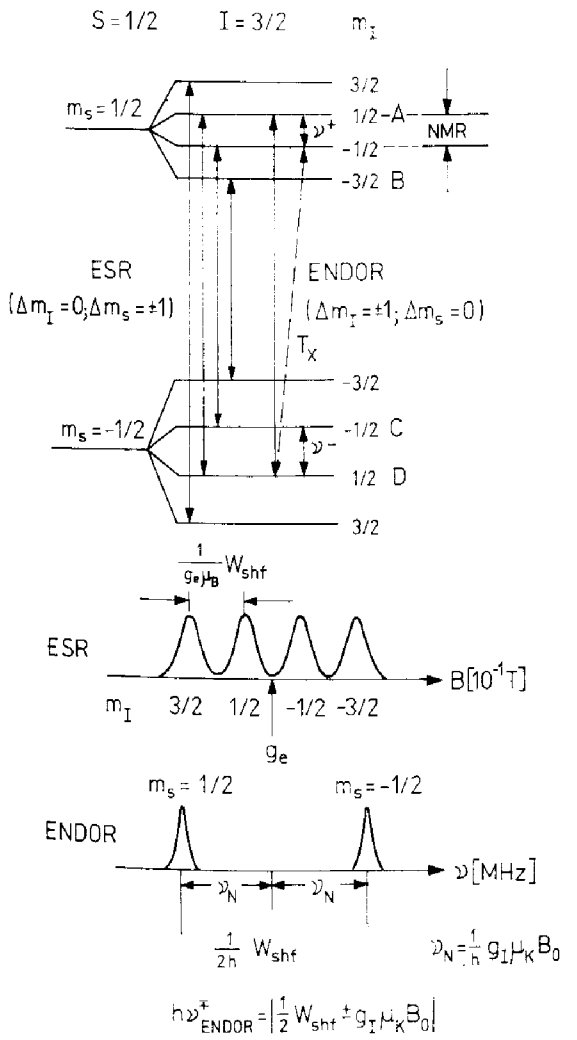

1

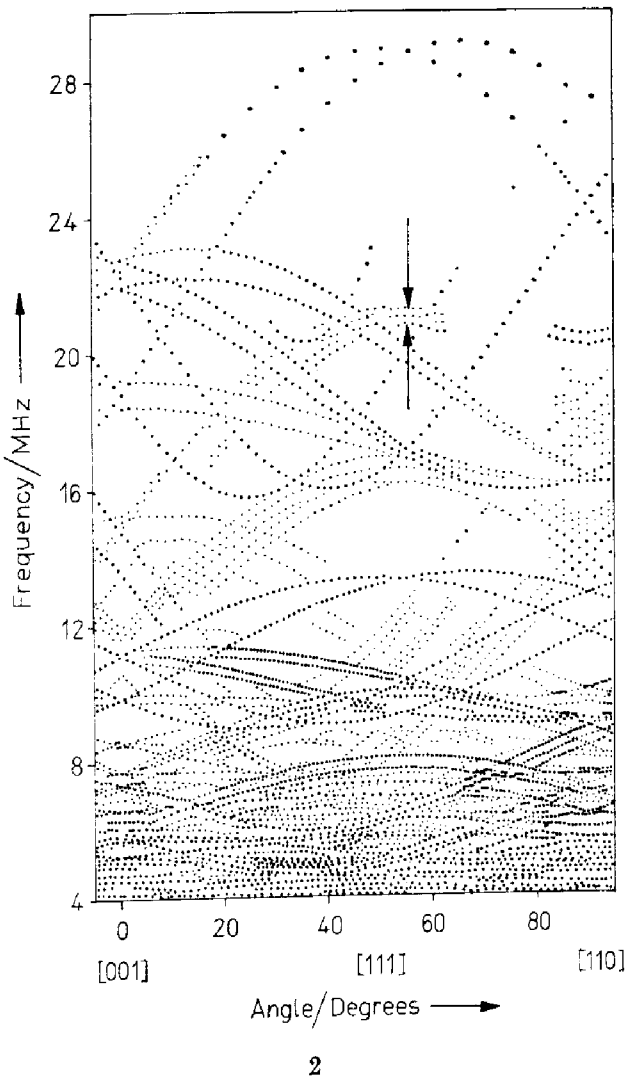

2

Fig. 1. Schematic representation of stationary ENDOR for the simplified system of $S = 1/2$ having a hyperfine interaction with one nucleus with $I = 3/2$

Fig. 2. ENDOR angular dependence of Ni^{3+} defects in GaP. ENDOR line positions for different ^{69}Ga and ^{71}Ga neighbours are below 22 MHz. The arrows mark the small Ga quadrupole interactions along [111]. After [4]

angular steps. A full angular dependence can take up to 2···3 weeks of continuous measurement at low temperature, in some cases, when the signals are very weak, also much more time, if a lot of signal averaging has to be done. The frequency positions of the ENDOR lines are determined by applying a particular 'peak search' algorithm [5]. Often it is necessary to use digital filtering [6, 7] of the signals in order to improve the signal-to-noise ratio and to 'smooth' the lines before applying the peak search algorithm. Other algorithms like subtraction of a background signal or deconvolution procedures may be needed, in particular, if many lines occur in a small frequency range [5]. Fig. 3 shows an example for digital filtering and peak searching.

A typical problem in materials science is the simultaneous presence of several defects. If their EPR spectra overlap, the measured ENDOR spectra may contain ENDOR lines of several defects, which usually renders their analysis impossible or at least very difficult. However, by measuring a kind of excitation spectrum of each ENDOR line, the ENDOR-induced EPR spectrum, one can establish a correlation of the ENDOR lines of one defect and their EPR spectrum. In this method one monitors the intensity of particular ENDOR lines as a function of the magnetic field B_0,

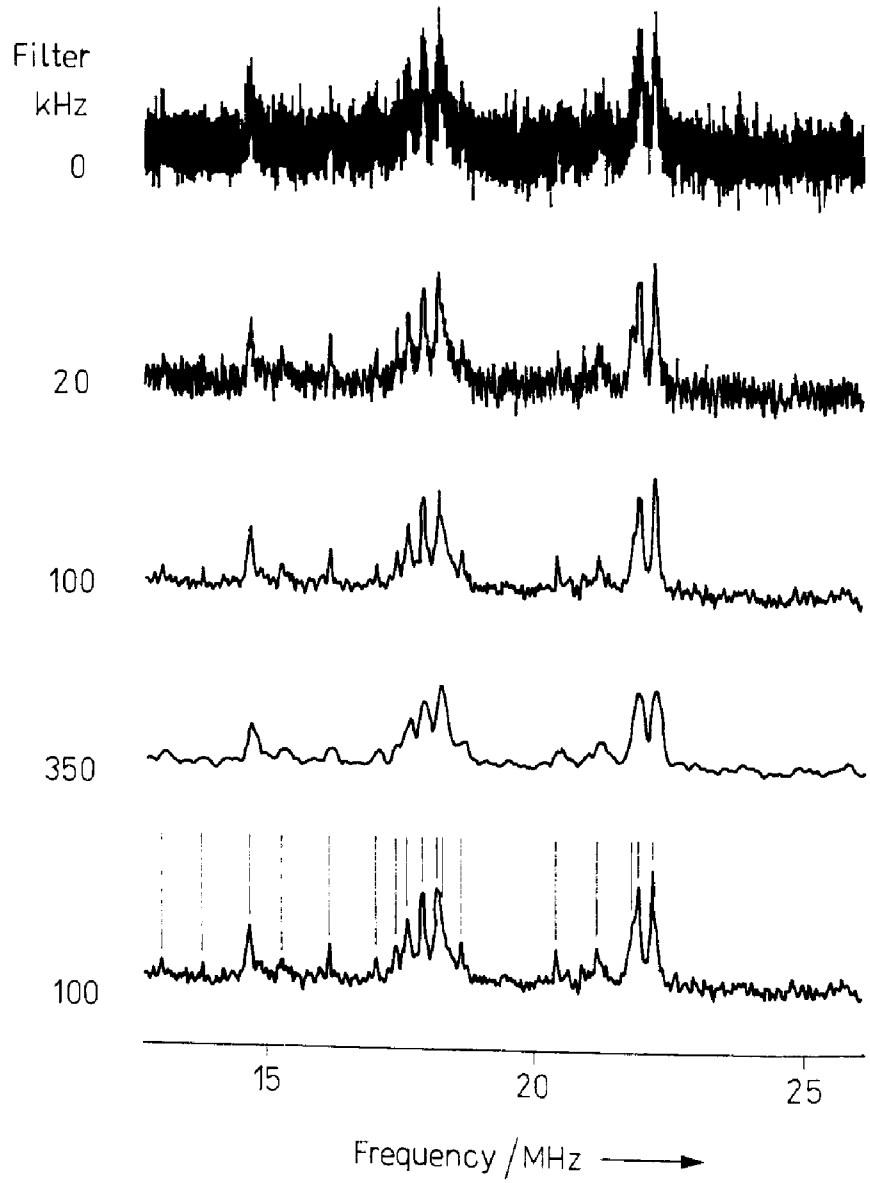

Fig. 3. Digital signal processing of ENDOR lines. Upper trace: stationary ENDOR as measured at X-band. The subsequent traces show the effect of the application of different digital filters with varying filter widths (in kHz). By the use of a 350 kHz filter structural information is lost, the filter is too broad. The digital filters conserve the first and second moments of the lines. The lowest trace shows the application of the peak search algorithm

which is varied through the EPR lines. The double resonance condition for each value of B_0 is maintained by driving the rf frequency accordingly and synchronously while sweeping B_0, which is possible, if the nuclear moment of the nucleus giving rise to the ENDOR line is known (see Fig. 1 for ENDOR double resonance condition). One then measures only that EPR spectrum (in 'integrated' form) of the defect to which the particular ENDOR line belongs. One can thus 'label' each ENDOR line [8, 9]. A more direct way to measure ENDOR of only one defect is to perform DOUBLE ENDOR experiments. Two NMR frequencies are applied simultaneously, together with the microwaves. One ENDOR line is chosen and its intensity is monitored as a function of the second rf frequency with a double lock-in technique. There is a signal only if both NMR transitions are indeed on nuclei belonging to the same defect, since their ENDOR transitions influence each other [10]. As an example, Fig. 4 shows the

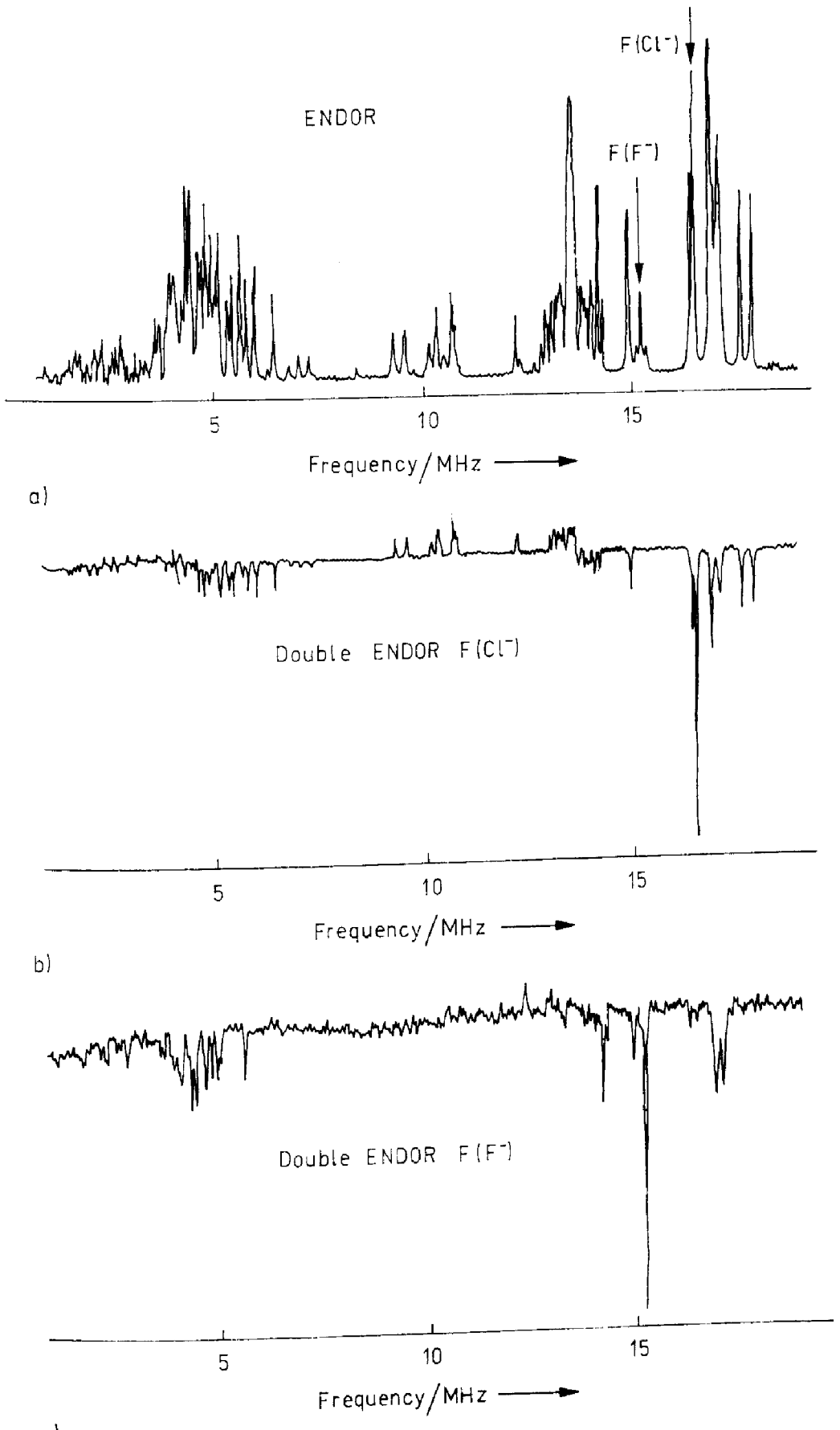

Fig. 4. ENDOR and DOUBLE ENDOR of two types of F centres in BaFCl.
a) Part of the ENDOR spectrum of $F(Cl^-)$ and $F(F^-)$ centres for B_0 15° off c in the c-a plane.
b) DOUBLE ENDOR spectrum for setting one ENDOR frequency to an ENDOR line of $F(Cl^-)$ centres.
c) DOUBLE ENDOR spectrum for setting one ENDOR frequency to an ENDOR line of $F(F^-)$ centres. After [11]

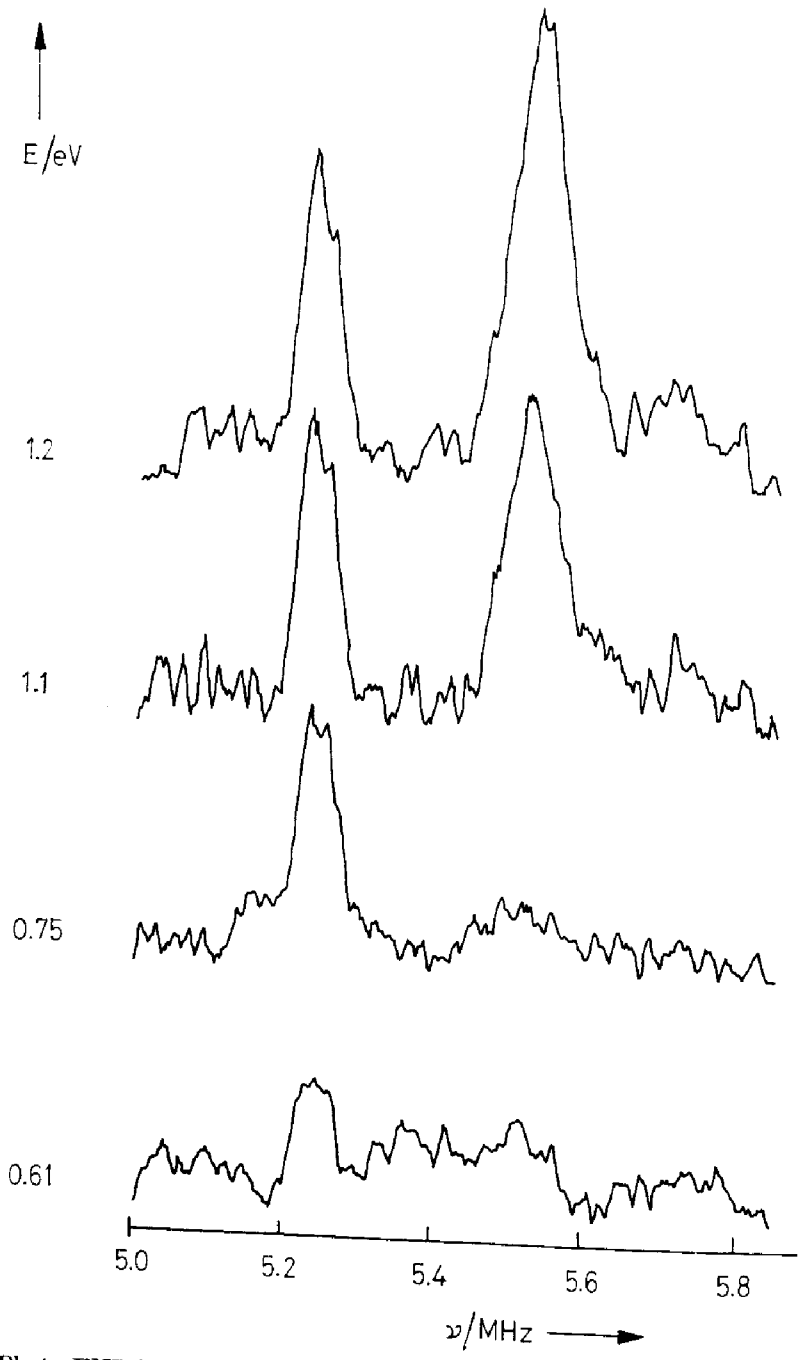

Fig. 5. Photo-ENDOR of S^+ and $(S—S)^+$ defects in Si. $T = 17$ K, X-band. After [14]

ENDOR (Fig. 4a) and DOUBLE ENDOR spectra (Fig. 4b and c) of a BaFCl crystal, which contains simultaneously two types of F-centres: F(Cl^-)-centres, in which the unpaired electron occupies a Cl^--vacancy, and F(F^-)-centres, in which the unpaired electron occupies an F^--vacancy [11]. In this stationary DOUBLE ENDOR spectrum positive and negative signals occur, which is qualitatively understood [12, 13]. The ENDOR lines around 5 MHz in BaFCl with both F-centres could never have been analyzed without the DOUBLE ENDOR technique.

In semiconductors a correlation of the ENDOR spectra of defects with their energy levels in the energy gap is particularly important. Mostly the energy levels of defects are determined by DLTS or related techniques, which, however, cannot identify the nature of a defect, while on the other hand 'only' EPR/ENDOR identification of a defect does not unravel their electric or optical properties, which depend on the energy level position. Such a correlation can be achieved by measuring two kinds

of crystals: one, in which the level of the defect in question is occupied by an unpaired electron and another one, where the Fermi energy is lower (e.g. by pinning the Fermi level at shallow acceptors), so that the level is empty. In the former, the EPR/ENDOR analysis is performed. The latter shows neither EPR nor ENDOR signals unless illuminated with light of sufficient energy such that electrons are raised from the valence band to occupy the level. Fig. 5 shows such a photo-ENDOR experiment in silicon doped with S. The crystal contained two paramagnetic defects: S^+ and $(S—S)^+$ pairs. The EPR/ENDOR signals of S^+ began to appear for light with $h\nu >$ 0.58 eV, while those of $(S—S)^+$ appeared for $h\nu > 0.8$ eV. In Fig. 5 for $h\nu = 0.75$ eV clearly only one kind of ENDOR signal (S^+) is measured [14]. The two levels identified at $E_c - (0.59 \pm 0.005)$ eV and $E_c - (0.37 \pm 0.05)$ eV agree well with those determined by optical spectroscopy [15].

Apart from the correlation the method can be used to separate the spectra of the two defects, the ENDOR lines of which strongly overlap in the same frequency range.

3. Optically Detected Electron Paramagnetic Resonance (ODEPR)

ODEPR measured in the optical emission has been a standard tool in the study of organic crystals within the properties of excited triplet states. It was also often used in semiconductor physics detecting EPR in donor-acceptor recombination luminescence. However, due to exchange coupling between donors and acceptors a resolution of a hf structure is only seldom possible and usually only broad, featureless EPR spectra are measured. A big advantage over conventional EPR is, however, the much higher sensitivity and selectivity and the possibility to correlate optical and structure properties [16]. Recently, however, the detection of EPR and ENDOR using the magnetic circular dichroism (MCD) of the optical absorption has proved to be a very useful method for materials science detecting ground state EPR/ENDOR with high sensitivity and selectivity and allowing correlations between structure and other bulk properties of the material. Although the method is known for a long time from colour centre physics [17], its application to semiconductors and impurity-doped insulating crystals is rather recent. Novel features have emerged, of which not all are well understood up to now.

In Fig. 6 the method is indicated schematically for an optical s-p-intracenter transition for $T = 0$. The MCD is the difference of the absorption constant of right and left circularly polarized light. If the absorption comes from a Kramers doublet with $S = 1/2$, one obtains [17]

$$\mathrm{MCD} = \frac{1}{2}\alpha_0 d \frac{\sigma_+ - \sigma_-}{\sigma_+ + \sigma_-} \frac{n_- - n_+}{n_- + n_+} \tag{1}$$

where α_0 is the absorption constant of unpolarized light, σ_+ and σ_- are the cross sections for right and left circular polarized light, respectively, n_+ and n_- are the occupation numbers for the $M_S = \pm 1/2$ states, d is the crystal thickness. The MCD effect is proportional to the occupation difference in the ground-state Zeeman levels $M_S = \pm 1/2$ and is a function of the spin orbit splitting $\Delta_{s.o.}$ of the excited states:

$$\mathrm{MCD} \propto \frac{n_- - n_+}{n_- + n_+} f(\Delta_{s.o.}). \tag{2}$$

The occupation difference is given by the Brillouin function for arbitrary S. For $S = 1/2$ the Brillouin function reduces to essentially $\tanh(g\beta_e B_0/2kT)$, thus is dependent on B/T. It is therefore advantageous to measure the MCD at low temperature (usually under 'pumped helium' condition at 1.5 K) and high filed ($B < 7$ T). Since for EPR

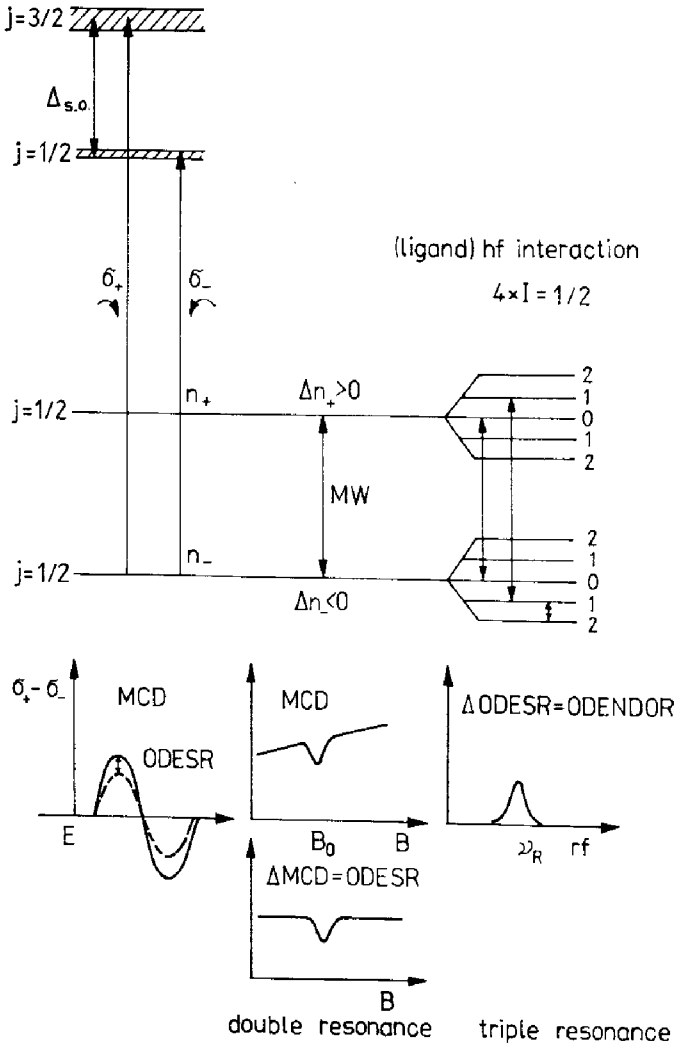

Fig. 6. Schematic representation of the optical detection of the ground state EPR and ENDOR of a Kramer's doublet via the microwave-induced change of the magnetic circular dichroism of an "atomic" s-p-transition with spin orbit splitting in the excited state. $T = 0$ K

small changes in the MCD must be measured and the MCD is proportional to $1/T$ at low temperature, temperature drifts or fluctuations must be avoided. This requires a control unit for the helium-vapour pressure, since microwaves and rf power dissipation changes the vapour pressure.

By using a stress modulator to produce right and left circular polarized light alternating in each half cycle at the modulator frequency of about 30 kHz and using lock-in technique to measure the difference in absorption of right and left circular polarized light, changes of the MCD of about 10^{-5} can be measured at an optical density of approx. 1.

With this modulation technique the MCD can be detected even when the optical absorption cannot be seen in a conventional direct experiment. Fig. 7 shows the optical absorption measured in undoped semi-insulating LEC-grown GaAs. The weak absorption band at 1.2 eV is due to diamagnetic EL2 defects. The MCD of paramagnetic $EL2^+$ defects (curve 1, Fig. 7b) is about 1% in its maximum and appears where the absorption is too weak to be detected directly. The concentration of $EL2^+$ defects was about 10^{16} cm^{-3} [18]. In order to measure EPR of the ground state, microwave transitions are induced between the ground state Zeeman levels. At a given temperature the occupation difference is reduced if the microwave transition rate is fast enough compared to the spin lattice relaxation rate, which at the usually used tem-

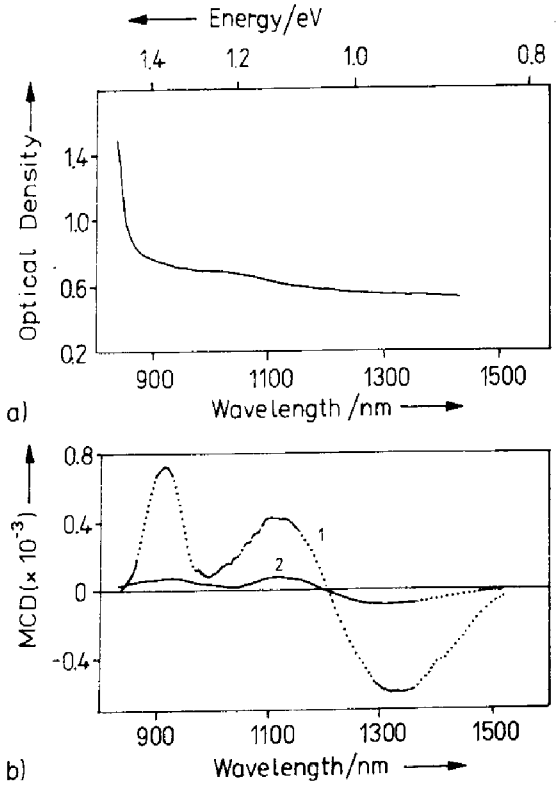

Fig. 7. a) Optical absorption of "as-grown" semi-insulating GaAs (crystal thickness 0.3 mm) at $T = 1.4$ K.
b) Curve 1: Magnetic circular dichroism (MCD) of the absorption of "as-grown" semi-insulating GaAs. $T = 4.2$ K, $B = 2$ T. Curve 2: Excitation spectrum of the optically detected EPR lines of the $EL2^+$ defects (MCD tagged by EPR). After [18]

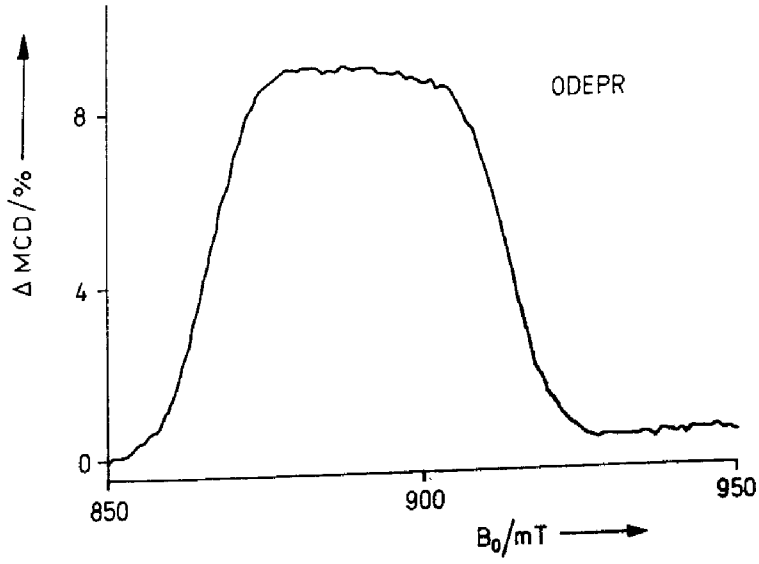

Fig. 8. ODEPR spectrum of V_{Ga}^{3+} defects in high resistivity GaAs measured at $h\nu = 1.1$ eV. ($g = 1.96 \pm 0.01$, $\nu_{ESR} = 24.41$ GHz, $T = 1.5$ K). After [19]

perature of 1.5 K is only small. The reduced occupation difference causes a reduction in the MCD, which is monitored. If there is a hf splitting, then the MCD reduction is smaller, since only spin packets of a particular nuclear spin quantum state take part in the occupation transfer (selection rule $\Delta M_I = 0$, $\Delta M_S = \pm 1$) (see also Fig. 6). Therefore, hf interactions can be resolved.

A recent ODMR spectrum is that of V^{3+} on Ga sites in s.i. GaAs (Fig. 8). The EPR line contains an unresolved hf splitting with ^{51}V ($I = 7/2$) into 8 lines, which is seen clearly in the line shape, which would be Gaussian in the absence of this interaction [19]. The ESR line shape and line width agree exactly with that measured in conventional EPR. V^{3+} is a $3d^2$ configuration with $S = 1$. The spin state was shown to be $S = 1$ by conventional ENDOR experiments [20], thus confirming the assumed charge state to be indeed V^{3+}. Also the hf and shf interactions could be resolved [20]. One of the interesting features of measuring the EPR spectra via the MCD is, that one can measure an MCD excitation spectrum of the EPR spectrum by setting the EPR resonance conditions to a particular EPR line and varying the optical wavelength and monitoring the ODEPR signal intensity as microwave-induced change of the MCD. Thus, from the total MCD of a sample one measures in this way only that part, which belongs to the particularly chosen EPR signal. This is particularly useful if a superposition of optical absorptions due to several defects is present, a typical case for e.g. radiation damage and impurity problems. Fig. 9 shows such an ODMR-MCD spectrum (MCD tagged by EPR [21]) for V_{Ga}^{3+} in GaAs). It only represents those MCD transitions, which belong to the V_{Ga}^{3+} defect. There are several zero phonon lines resolved and the intracenter transitions $^3A_2 - {}^3T_1$ into Jahn/Teller split excited states [22] are clearly seen. This measurement provides a unique possibility to safely associate all the features of the optical spectra to one particular defect irrespective of the presence of other defects in the crystal as long as the EPR spectra of different defects do not completely overlap.

Since one can vary the crystal orientation and thus select a particular defect orientation via the EPR lines, it is also possible to obtain information about the polarization properties of the different optical absorption transitions. This cannot be

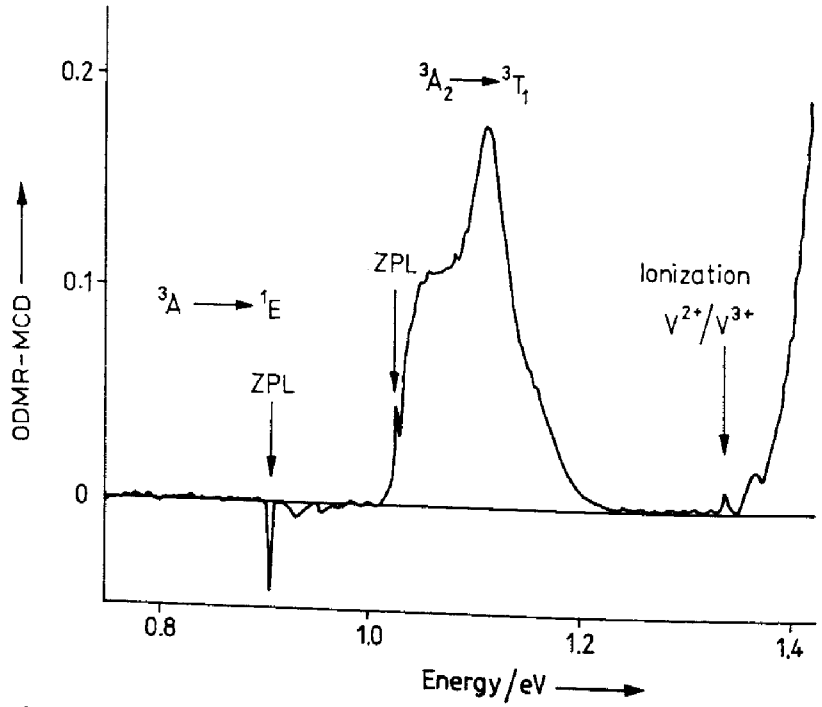

Fig. 9. Excitation spectrum of the ODEPR lines of V_{Ga}^{3+} in high resistivity GaAs. (MCD tagged by EPR), $T = 1.6$ K. After [19]

obtained, if the absorption bands are hidden under optical absorptions of other defects. A good example for this was recently obtained by studying $Tl^0(1)$, $Ga^0(1)$ and $In^0(1)$ centres in alkali halides, which are axial centres (neutral metal atom next to an anion vacancy), produced by electron irradiation. $Tl^0(1)$ centres are laser-active [21, 23].

A particularly interesting novel feature is the fact, that the ODEPR could also be measured in the ionizing transition around about 1.4 eV, which is a hole transition into the valence band (Fig. 9). Similarly, ODEPR could be observed recently in InP: Fe^{3+} in an ionizing transition to the conduction band [19]. This is a remarkable feature, since if this is generally true, one does not need the existence of an intracenter optical absorption to measure ODEPR. Why the EPR can be observed in a transition into the edge of a band, is not yet fully clear. Perhaps one can rationalize the experimental finding in the following way: the transition occurs into a defect-induced state resonant with the band, which contains the spin orbit interaction necessary to observe an MCD. Since the optical transition occurs in the time regime of femto seconds and phonons may destroy the states only in the time regime of pico seconds, this defect-induced resonant state lives long enough for the MCD to be observed before the charge carriers are thermalized in the band. The experimental results suggest, that there is a continuum of such states. The fact that the carriers are thermalized after the transition is experimentally seen in the result, that no optical pumping can be achieved.

For the determination of the charge state of a defect it is important to know its spin state. Its determination is normally not easy from EPR spectra unless there is a fine structure splitting resolved in a multi-electron system. Otherwise, one has to resort to ENDOR. However, using the MCD technique, there is yet another way to determine the spin state, as was discovered recently [19]. Fig. 10 shows the ODEPR spectrum of V_{Ga}^{2+} in an inhomogeneous semi-insulating GaAs sample. V_{Ga}^{2+} has a $3d^3$ configuration and has a similar line shape as V^{3+} due to unresolved ^{51}V hf structure. Its spin state should be $S = 1/2$, that is low spin, according to recent theoretical predictions [24, 25]. This cannot be inferred from the EPR spectrum. The MCD is composed of a diamagnetic and a paramagnetic term:

$$\mathrm{MCD} = \mathrm{MCD_{dia}} + \mathrm{MCD_{para}}. \tag{3}$$

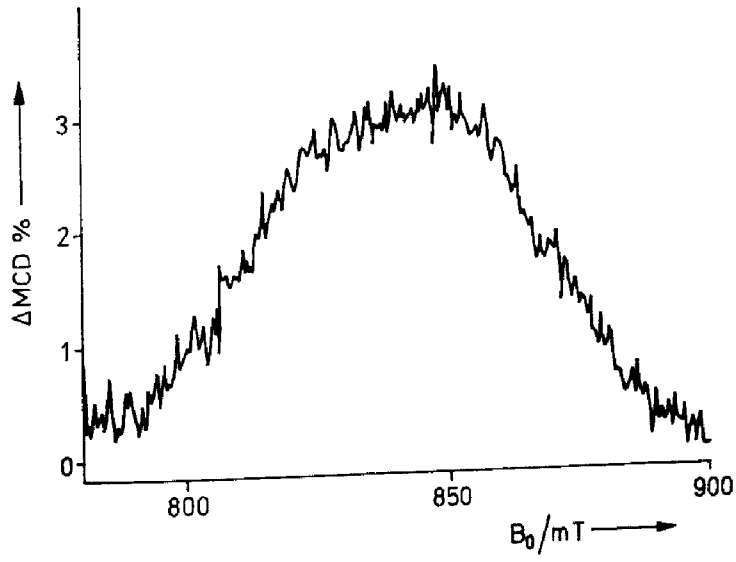

Fig. 10. ODEPR spectrum of the V_{Ga}^{2+} defect in high resistivity (n-type) GaAs. (Measured at $h\nu = 1.25$ eV, $g = 2.07 \pm 0.02$, $\nu_{ESR} = 24.42$ GHz, $T = 1.5$ K). After [19]

The diamagnetic term is proportional to the magnetic field B_0 and is usually small compared to the paramagnetic part MCD_{para}.

The latter is proportional to the Brillouin function B_S and the spin

$$MCD_{para} \propto S \cdot B_S(g, S, B_0/T). \tag{4}$$

If the ground state does not mix appreciably with the excited states (that means that g is near $g = 2$) one can perform the following measurements:

One measures the MCD for several pairs of B_0 and T values and forms the following ratio:

$$R_{exp} = \frac{MCD(B_1, T_1) - MCD(B_1, T_2)}{MCD(B_2, T_1) - MCD(B_2, T_2)} \tag{5}$$

Since the diamagnetic term cancels, this gives

$$R(S) = \frac{B_S(S, B_1/T_1) - B_S(S, B_1/T_2)}{B_S(S, B_2/T_1) - B_S(S, B_2/T_2)} \tag{6}$$

Eq. (6) can be calculated theoretically varying spin S. Thus, the spin of the defect is determined, when the condition $R_{exp} = R(S)$ is fulfilled. In eq. (6) the experimental g-value is inserted. Fig. 11 shows the comparison of $R_{exp}/R(S)$ for V_{Ga}^{2+} in GaAs: agreement between R_{exp} and $R(S)$ is indeed obtained for $S = 1/2$, that is for a low

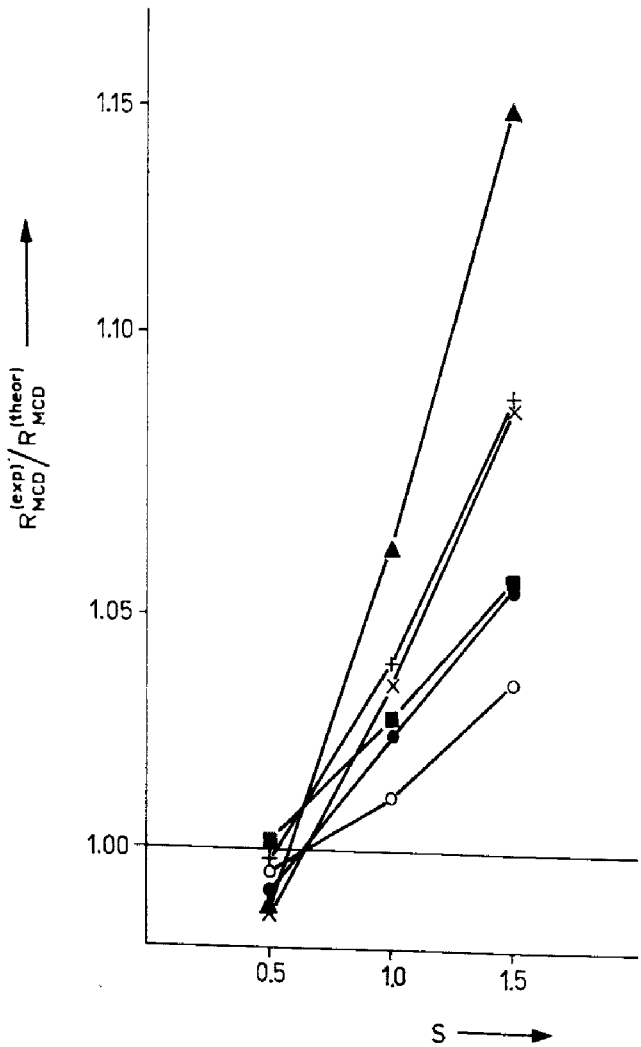

Fig. 11. Ratio of R_{exp} and R_{calc} (S) as a function spin S for V_{Ga}^{2+} measured at 1.25 eV in n-type GaAs: V for the following pairs of magnetic field values: B_1 and B_2 (in T) (1.3 and 0.5), (1 and 0.8), (0.8 and 0.5) at temperatures $T_1 = 1.65$ and $T_2 = 4.2$ K. After [19]

spin state. This is the first observation of a transition metal low spin state in a semiconductor. The method works equally well for V_{Ga}^{3+} and confirms once more $S = 1$, which was already known from ENDOR [19].

4. Optically Detected ENDOR (ODENDOR)

The method of optical detection via the MCD recently proved to be very appropriate for resolving shf interactions by ENDOR. Fig. 6 shows schematically the principle of this experiment for the case of shf interactions with 4 equivalent neighbours with nuclear spin $I = 1/2$. The EPR selection rule $\Delta M_I = 0$ implies, that only a fraction of the spin packets can decrease the MCD, since the microwaves induce transitions only between a particular combination of $M_{I,1}$ states. If an additional NMR frequency is simultaneously applied, which combines the $M_{I,1}$ states with its neighbouring ones, then more spin packets are shifted into the microwave pump channel and contribute to the decrease in MCD. Thus, with such an NMR resonance, the decrease of the MCD is enhanced, and this is monitored [26]. Fig. 12 shows a section of the ODENDOR spectrum of $EL2^+$ defects in semi-insulating 'as-grown' GaAs. The ENDOR lines are due to five ^{75}As nuclei. The $EL2^+$ defect consists of a singly ionized atom on a Ga-site, As_{Ga}^+, which is paramagnetic, paired with a diamagnetic interstitial As_i^+ along a [111] direction, it is thus a $(As_{Ga}^+ - As_i^+)$ pair defect. The ENDOR lines of Fig. 12 are due to the 4 nearest As-ligands of the As_{Ga}^+-antisite and due to the As_i^+-interstitial [27]. They are measured as rf-induced changes of the ODEPR lines, which consist of a hf split quadruplet due to the interaction of the unpaired electron with the central ^{75}As nucleus ($I = 3/2$).

Unlike in conventional solid state defect ENDOR, it was found that the ODENDOR effect can be as big as the ODEPR effect. This was in particular observed for the $EL2^+$ centres in GaAs. Fig. 13 shows the ENDOR effect measured through one of the 4 ^{75}As hf EPR lines of the $EL2^+$ defect. In the flank of the EPR line both effects are about equal [28]. This is, apart from the sensitivity enhancement through optical detection, a great advantage compared to conventional ENDOR. The ENDOR effect is not always as big as in the case of the EL2 centres. For P antisite defects

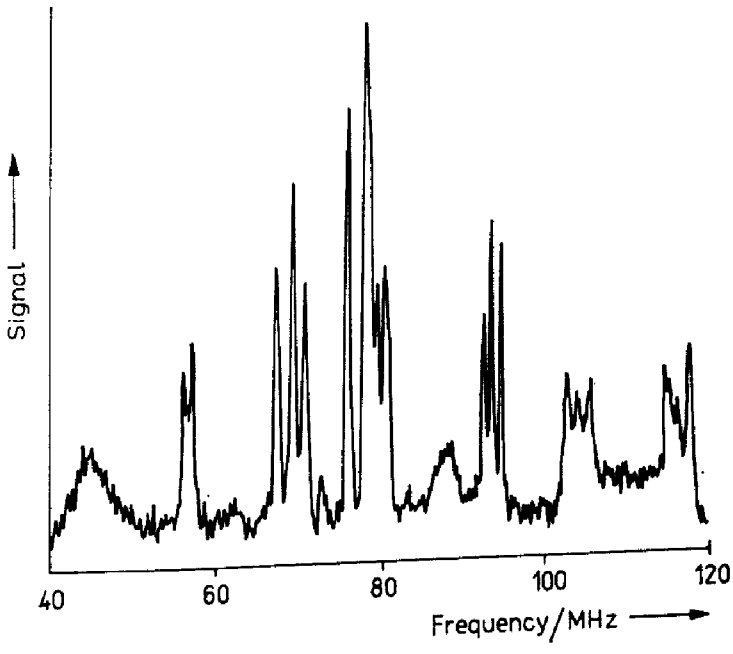

Fig. 12. Section of the ODENDOR spectrum of $EL2^+$ defects in semi-insulating GaAs. $T = 1.5$ K, with B_0 in a (110) plane. The lines are due to 5 ^{75}As neighbours of the As_{Ga}^+. After [27, 28]

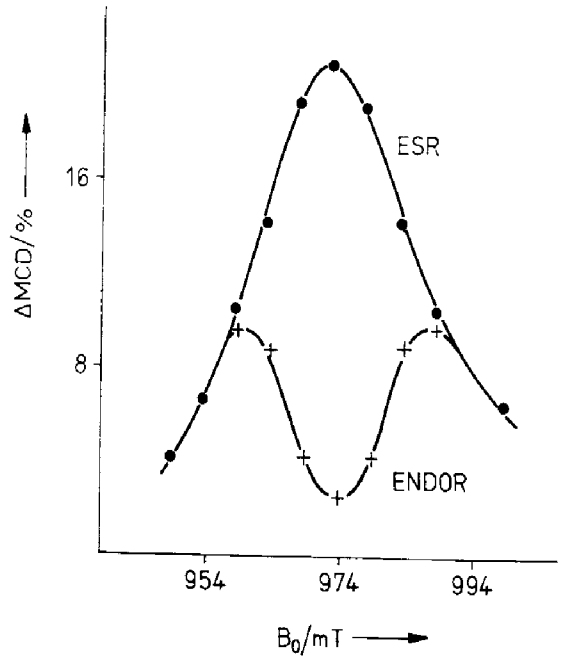

Fig. 13. Size of the ODEPR and ODENDOR effects measured in the high field ODEPR line of the $EL2^+$ defect in semi-insulating "as-grown" GaAs. After [28]

in GaP it was found to be only about 3 % of the EPR effect [27], for V_{Ga}^{3+} in GaAs about 5···10 % [19]. It must be remarked, that the ODENDOR effect is not yet understood quantitatively, in particular not what was observed for the $EL2^+$ centres in GaAs. The decrease of the MCD in each of the 4 ^{75}As hf ODEPR lines is about 20 %, suggestive of homogeneous EPR lines, since the total change of the MCD amounts to approximately 80 %. As the ODENDOR measurements showed, however, the EPR lines are inhomogeneously broadened: as small interactions as a few MHz could be resolved for the twelve 3rd-shell ^{75}As neighbours. Thus, if one tried to explain the ENDOR effect on the basis of the nuclear spin statistics, the ODEPR effect is too large by about 3···4 orders of magnitude. There is no good explanation yet for the observations. Possibly, dynamical nuclear polarization effects play an important role.

Similarly, as for ODEPR, the 'MCD tagged by ENDOR' can be measured, correlating optical bands with one single ENDOR line. Curve 2 in Fig. 7 b is the excitation spectrum of the EPR line, which has the same spectral shape as the excitation spetrum of the ENDOR line of the $EL2^+$ defects in GaAs proving, that the total MCD measured in s.i. as-grown GaAs is due to the $EL2^+$ defects. With this technique details of a defect structure as revealed in a single ENDOR line can be correlated with optical properties of the defect.

As for conventional EPR/ENDOR, also photo-ODEPR/ODENDOR experiments can be performed by using p-type samples with empty defect levels and occupying them from the valence band by an additional light source, thus performing triple (photo-ODEPR) and quadrupole (photo-ODENDOR) experiments. In this way it could be established, that the ODENDOR spectra of the $EL2^+$ defects are indeed correlated with the level known from DLTS of the singly ionized EL2 [27].

5. Conclusions

Magnetic multiple resonance methods are a very powerful tool for the investigation of defects in materials science. The availability of modern experimental techniques

makes it possible to tackle difficult problems of interest in materials development. The development of these methods is by no means complete. The optical detection of EPR/ENDOR allows, e.g. to perform spatially resolved experiments. First results of the distribution of $EL2^+$ and $EL2^0$ defects were obtained for s.i. GaAs across a wafer [29]. Time resolved experiments will allow not only to study dynamical phenomena, but also to use the donor-acceptor luminescence to detect EPR/ENDOR with better hf resolution. The increase in sensitivity can be driven further, which is of particular interest for defect investigations in thin layers.

References

[1] Feher, G., Phys. Rev. **114** (1959) 1219, 1249.
[2] Seidel, H., Z. Physik **165** (1962) 218, 239.
[3] Hoentzsch, Ch.; Niklas, J. R.; Spaeth, J.-M., Rev. Sci. Instrum. **49** (1978) 1100.
[4] Ueda, Y.; Niklas, J. R.; Spaeth, J.-M.; Kaufmann, U.; Schneider, J., Solid State Commun. **46** (1983) 127.
[5] Niklas, J. R., Habilitationschrift, Paderborn 1983.
[6] Bromba, M. U. A.; Ziegler, H., Anal. Chem. **55** (1983) 648.
[7] Bromba, M. U. A.; Ziegler, H., Anal. Chem. **56** (1984) 2052.
[8] Niklas, J. R.; Spaeth, J.-M., phys. stat. sol. (b) **101** (1980) 221.
[9] Spaeth, J.-M.; Niklas, J. R., Recent Developments in Condensed Matter Phys. **1** (1981) 393.
[10] Biehl, R.; Plato, M.; Möbius, K., J. Chem. Phys. **63** (1975) 3515.
[11] Bauer, R. U.; Niklas, J. R.; Spaeth, J.-M., phys. stat. sol. (b) **118** (1983) 557.
[12] Dalal, N. S.; McDowell, C. A., Chem. Phys. Lett. **6** (1970) 617.
[13] Niklas, J. R.; Bauer, R. U.; Spaeth, J.-M., phys. stat. sol. (b) **119** (1983) 171.
[14] Greulich-Weber, S., Dissertation, Paderborn 1987.
[15] Wagner, P.; Holm, C.; Sirtl, E.; Oeder, R.; Zulehner, W., Festkörperprobleme: Advances in Solid State Physics, ed. P. Grosse (Vieweg, Braunschweig, 1984), XXIV, 191.
[16] Cavenett, B. C., Advances in Physics **30** (1981) 475.
[17] Mollenauer, L. F.; Pan, S., Phys. Rev. **B6** (1972) 772.
[18] Meyer, B. K.; Spaeth, J.-M.; Scheffler, M., Phys. Rev. Lett. **52** (1984) 851.
[19] Görger, A., Diplomarbeit, Paderborn 1987.
[20] Hage, J.; Niklas, J. R.; Spaeth, J.-M., J. Electron. Mat. **14a** (1985) 1051.
[21] Ahlers, F. J.; Lohse, F.; Spaeth, J.-M.; Mollenauer, L. F., Phys. Rev. **B28** (1983) 1249.
[22] Ulrici, W.; Friedland, K.; Eaves, L.; Halliday, D. P., phys. stat. sol. (b) **131** (1985) 719.
[23] Ahlers, F. J.; Lohse, F.; Hangleiter, Th.; Spaeth, J.-M.; Bartram, R. H., J. Phys. C **17** (1984) 4877.
[24] Katayama-Yoshida, H.; Zunger, A., Phys. Rev. **B33** (1986) 2961.
[25] Fazzio, A.; Caldaus, M. J.; Zunger, A., Phys. Rev. **B30** (1984) 3430.
[26] Hofmann, D. M.; Meyer, B. K.; Lohse, F.; Spaeth, J.-M., Phys. Rev. Lett. **53** (1984) 1187.
[27] Meyer, B. K.; Hofmann, D. M.; Niklas, J. R.; Spaeth, J.-M., Phys. Rev. **B36** (1987) 1332.
[28] Hofmann, D. M., Dissertation, Paderborn 1987.
[29] Heinemann, M.; Meyer, B. K.; Spaeth, J.-M.; Löhnert, K., Proc. Internat. Symp. DRIP II, Monterey, USA, 1987.

Prof. Dr. Johann-Martin Spaeth, Universität-GH-Paderborn, FB 6 Physik, Warburger Str. 100A, D - 4790 Paderborn.